Depletion of Peripheral Macrophages and Brain Microglia Increases Brain Tumor Titers of Oncolytic Viruses

Giulia Fulci,[1,2,6] Nina Dmitrieva,[6] Davide Gianni,[1] Elisabeth J. Fontana,[1] Xiaogang Pan,[7] Yanhui Lu,[7] Claire S. Kaufman,[4] Balveen Kaur,[6] Sean E. Lawler,[6] Robert J. Lee,[7] Clay B. Marsh,[8] Daniel J. Brat,[9] Nico van Rooijen,[10] Anat Stemmer Rachamimov,[1,3] Fred H. Hochberg,[5] Ralph Weissleder,[4] Robert L. Martuza,[2] and E. Antonio Chiocca[1,6]

[1]Molecular Neuro-oncology Laboratories, Neurosurgery Service, and Center for Molecular Imaging, Massachusetts General Hospital, Charlestown, Massachusetts; [2]Brain Tumor Research Center, Neurosurgery Service, and Departments of [3]Pathology, [4]Radiology, and [5]Neurology, Massachusetts General Hospital, Boston, Massachusetts; [6]Department of Neurological Surgery, Dardinger Laboratory for Neuro-oncology and Neurosciences, James Cancer Hospital/Solove Research Institute, [7]Division of Pharmaceutics, College of Pharmacy, and [8]Department of Internal Medicine, The Ohio State University Medical Center, Columbus, Ohio; [9]Department of Pathology and Laboratory Medicine, Emory University School of Medicine, Atlanta, Georgia; and [10]Department of Cell Biology and Immunology, Vrije Universiteit, Amsterdam, the Netherlands

Abstract

Clinical trials have proven oncolytic virotherapy to be safe but not effective. We have shown that oncolytic viruses (OV) injected into intracranial gliomas established in rodents are rapidly cleared, and this is associated with up-regulation of markers (CD68 and CD163) of cells of monocytic lineage (monocytes/microglia/macrophages). However, it is unclear whether these cells directly impede intratumoral persistence of OV through phagocytosis and whether they infiltrate the tumor from the blood or the brain parenchyma. To investigate this, we depleted phagocytes with clodronate liposomes (CL) *in vivo* through systemic delivery and *ex vivo* in brain slice models with gliomas. Interestingly, systemic CL depleted over 80% of peripheral CD163$^+$ macrophages in animal spleen and peripheral blood, thereby decreasing intratumoral infiltration of these cells, but CD68$^+$ cells were unchanged. Intratumoral viral titers increased 5-fold. In contrast, *ex vivo* CL depleted only CD68$^+$ cells from brain slices, and intratumoral viral titers increased 10-fold. These data indicate that phagocytosis by both peripheral CD163$^+$ and brain-resident CD68$^+$ cells infiltrating tumor directly affects viral clearance from tumor. Thus, improved therapeutic efficacy may require modulation of these innate immune cells. In support of this new therapeutic paradigm, we observed intratumoral up-regulation of CD68$^+$ and CD163$^+$ cells following treatment with OV in a patient with glioblastoma. [Cancer Res 2007;67(19):9398–406]

Introduction

Oncolytic viruses (OV) for cancer therapy are interesting because they replicate selectively within tumor cells, thereby leading to successive rounds of viral replication and increased intratumoral OV titers (1–9). However, clinical trials have shown OV to be safe but not effective (10–17), possibly because viral replication was less than anticipated. In fact, OV can kill tumor cells grown *in vitro* with high efficiency (i.e., with input multiplicity of infection of 0.001–0.1). Yet, the same viruses used *in vivo* to treat tumors derived from the same cancer cells are less effective; large and sometimes repeated doses of OV are required to show significant biological effects. Thus, OV efficacy seems impeded by tumoral and/or host factors.

Rapid patient response to viral therapy, including increased intratumoral numbers of immune cells and/or acute-phase systemic reaction, has been described, but the mechanism/s underlying these responses is/are unclear (14). Initially, OVs were believed to vaccinate the host against cancer by initiating adaptive immunity (18–23). However, early innate immune responses may actually inhibit successful virotherapy (24–36). For example, immunomodulation by cyclophosphamide (CPA) rapidly intensifies OV ability to infect and destroy brain tumors, reducing tumor volume and prolonging survival in immunogenic and athymic rodents harboring gliomas (24, 27, 31). Similar responses in both animal models suggest mediation of this effect by innate immune responses rather than T-cell–mediated adaptive immunity.

Immunohistochemical analysis of gliomas treated with OV has shown intratumoral clearance of over 80% of viral particles shortly after delivery, associated with up-regulation and infiltration of cells of monocytic lineage (31, 32). This was observed in a glioma model in immunocompetent rats treated with a herpes simplex virus (HSV)-derived OV (31) and in a human glioblastoma model in nude mice treated with an adenovirus-derived OV (32). Thus, this phenomenon seems neither species nor virus specific.

We have hypothesized that early intratumoral viral clearance results from phagocytosis by cells of monocytic origin that infiltrate tumor following OV delivery and that transient depletion of these cells during OV delivery would help intratumoral propagation and persistence of virus, thereby rendering more efficient therapy. We herein explore the validity of this hypothesis by analyzing how depleting systemic phagocytic cells or brain-resident microglia affects intratumoral OV delivery.

Materials and Methods

Viruses, cells, and chemicals. hrR3 is an OV derived from HSV1 with an *Escherichia coli LacZ* gene inserted in the *ICP6* locus (37). D74/HveC (27) rat glioma cells were grown in complete DMEM supplemented with 7.5 μg/mL blasticidin S (Calbiochem). Clodronate liposomes (CL) were prepared as

Note: Supplementary data for this article are available at Cancer Research Online (http://cancerres.aacrjournals.org/).

Requests for reprints: Giulia Fulci, Brain Tumor Research Center, Neurosurgery Department, Massachusetts General Hospital, Simches Research Building CRPZN 3800, 185 Cambridge Street, Boston, MA 02114. Phone: 617-643-3431; Fax: 617-643-3422; E-mail: gfulci@partners.org or E. Antonio Chiocca, Department of Neurological Surgery, The Ohio State University Medical Center, N-1017 Doan Hall, 410 West 10th Avenue, Columbus, OH 43210. Phone: 614-293-9312; Fax: 614-293-4024; E-mail: EA.Chiocca@osumc.edu.

doi:10.1158/0008-5472.CAN-07-1063

follows. A lipid mixture, composed of 1.2 g hydrogenated soya phosphatidyl choline (Lipoid) and 0.4 g cholesterol (Sigma-Aldrich) at a molar ratio of 6:4, was dissolved in 12 mL ethanol/tert-butanol (5:1, v/v). The solvent was removed by rotary evaporation in a round-bottomed flask. The resulting thin film of lipids was hydrated in 32 mL of 0.25 g/mL clodronate solution (gift from Farchemia). A trace amount of water-soluble fluorescent dye, calcein (Sigma-Aldrich), was added as an aqueous phase marker. To reduce particle size, the suspension of hydrated lipids was subjected to agitation and five cycles of freezing and thawing followed by homogenization on an Avestin Emulsiflex C-5 for 10 min at 10,000 p.s.i. To further restrict particle size distribution, the liposomes were serially extruded through 400- and 200-nm track-edge polycarbonate membranes. Tangential flow diafiltration on a Millipore Pellicon XL Labscale System was followed to obtain the liposomal product. Liposome size was determined by photo correlation spectroscopy using a NICOMP370 particle sizer (Particle Sizing Systems) to assess clodronate concentration in the liposome following disruption of the liposomes in 80% ethanol. Mean particle diameter was 181 $\pm$ 59.1 nm. Clodronate encapsulation efficiency was 16%, consistent with passive entrapment.

Animal studies. Male Fischer 344 rats and athymic *nu/nu* mice (Taconic) were kept according to the guidelines of the Subcommittee on Research Animal Care of the Massachusetts General Hospital. For tumor implantation, 2×10^5 rat glioma D74/HveC cells (27) were stereotactically injected into the right frontal lobes, 2.5 mm lateral from the Bregma and 4 mm deep from the surface (27). Tumors were grown for 5 days before i.p. treatment with 80 mg/kg CPA (Bristol-Myers Squibb) or 20 mg CL. CL treatment was repeated daily until day 3 after viral injection. Control rats were injected with 1 mL PBS at the same time the other animals received CL or CPA treatment. Seven days after implantation of glioma cells, 2×10^7 plaque-forming units (pfu) of hrR3 were injected intratumorally using the same procedure and stereotactic coordinates as for the tumor cells.

Magnetic resonance imaging. Rats were anesthetized with isoflurane (2.0–3.0% at 2 L/min) and imaged using a 4.7-T, 16-cm bore magnetic resonance (MR) imaging system (Bruker Pharmascan). Rats were imaged before and after i.v. injection of monocrystalline iron oxide 46 (10 mg/kg body weight) and at 24 h after injection. MR images included both T_2-weighted gradient echo sequence [repetition time (TR), 600 ms; echo time (TE), 6 ms; matrix size (MTX), 128 $\times$ 128; slice thickness, 0.8 mm; number of excitations (NEX), 8; and field of view (FOV), 3.5 cm] and multiple-slice multiple-echo sequence (TR, 2,000 ms; TE, 6.0–104.0 ms; MTX, 128 $\times$ 128; slice thickness, 0.8 mm; NEX, 8; and FOV, 3.5 cm). Tumor volumes were measured using a 4.7-T, 16-cm bore MR imaging system. Rats were injected i.v. with gadolinium-diethylenetriaminepentaacetic acid (600 μL/kg, Magnevist, Berlex Laboratories). Coronal and axial scans were taken using a T_1-weighted fast spin echo sequence (TR, 600 ms; TE, 4.4 ms; FOV, 4.0 $\times$ 4.0 cm; MTX, 192 $\times$ 192; slice thickness, 1.0 mm; 8 averages). The widths of the tumors were measured at three axes using Paravision software (Bruker Pharmascan) and approximating an ellipsoid shape.

Extraction and storage of tissues. For tissue analysis, rats were sacrificed 3 days after virus injection. Brains were extracted and frozen in an isopentane dry-ice bath and then sectioned using a cryostat through the entire tumor volume to a thickness of 6 μm. Every fifth section was analyzed. Tissue slides were dried overnight at room temperature, fixed for 10 min in ice-cold acetone, and stored at −20°C for immunohistochemical analysis. Spleen and peripheral blood were extracted from the same animals and analyzed by fluorescence-activated cell sorting (FACS) as described below.

Immunohistochemistry. Brain tissue slices were thawed and rehydrated 5 min in PBS before staining. The central and peripheral areas of tumors were analyzed for macrophage infiltration: endogenous proteins were blocked with serum-free protein block (DakoCytomation) and endogenous peroxidases with a peroxidase-blocking reagent (DakoCytomation). Sections were then incubated with the primary antibody for 1 h at room temperature and, after three washes in PBS, incubated with the secondary antibody at room temperature for 1 h. The primary antibodies used were mouse anti-rat CD68 and CD163 (Serotec), and the secondary antibodies were a horseradish peroxidase–conjugated anti-mouse IgG (enhanced chemiluminescence anti-mouse IgG; Amersham) and FITC-conjugated anti-mouse IgG (Jackson ImmunoResearch). DAKO Liquid DAB Substrate Chromogen System (DakoCytomation) was used to detect peroxidase. Peroxidase-labeled sections were counterstained with hematoxylin, dehydrated with increasing concentrations of ethanol, and fixed in xylene. Fluorescent sections were mounted with Vectashield medium containing 4′,6-diamidino-2-phenylindole (Vector 1200; Vector Laboratories) for nuclear counterstaining.

Flow cytometry analysis (FACS). Whole spleen or brain hemisphere was broken into single cells using a syringe plunger and filtrated through a 70-μm cell strainer. Erythrocytes were lysed using the Erythrolyse solution (Sigma-Aldrich), and the remaining cells were resuspended in PBS (10^6/100 μL PBS). Before staining with the CD68 antibody, the cells were made permeable using the Leucoperm kit (Serotec). Fifteen-minute treatment with anti-rat CD32 monoclonal antibody (BD Biosciences) inhibited Fc-mediated binding to FcgII receptors on rat splenocytes. Cells were then incubated with the primary antibody (anti-rat CD68 or CD163, FITC-conjugated antibodies; Serotec) in the dark for 45 min at room temperature, washed with 5 mL PBS, and resuspended in 400 μL 2% paraformaldehyde in PBS. The same staining procedure was applied for peripheral blood mononuclear cells, which were isolated from peripheral blood following plasma separation and lysis of erythrocytes with Erythrolyse solution. The fluorescence-labeled cells were counted using the FACSCalibur cytometer connected to CellQuest software (BD Biosciences).

***In vitro* culture and treatment of brain slices.** Organotypic brain slices were aseptically prepared from 5- to 7-day-old rats. Brains were rapidly excised and cut into 100-μm slices using a vibrotome (VT100 S, Leica). Slices were incubated at 36°C on a 0.4-μm polycarbonate membrane (Millipore) and fed with filtered MEM (50%), 25% fetal bovine serum, and 25% HBSS, L-glutamine (1 mmol/L), and D-glucose (36 mmol/L). Four weeks later, brain slices were treated with CL or PBS for 24 h, washed thoroughly, and cultured for 72 h before establishing D74/HveC rat glioma spheroids by the hanging drop method (38). Each spheroid was established by placing 2,000 glioma cells on the brain slices and allowing them to grow for 1 week before infection with 50 pfu of hrR3. The same procedure was applied for brain slices from 5- to 8-day-old athymic *nu/nu* mice implanted with human glioblastoma X12 cells (39) and infected with rQNestin34.5 HSV-derived OV (40).

The 100-μm brain slices were stained by immunofluorescence using the same antibodies as for immunohistochemistry, but the reactions occurred in suspension, and the primary antibody was incubated for 2 days at 4°C and the secondary antibody for 24 h at 4°C. Live isolectin staining was done by submerging the slices in an isolectin solution (5 μL/mL) in culture medium (Isolectin GS-IB4 from Griffonia simplicifolia, Alexa Fluor 488 conjugate; Molecular Probes).

Evaluation of intratumoral distribution of OV. To evaluate intratumoral propagation of OV, every fifth frozen brain tissue slide was rehydrated in PBS, stained with 5-bromo-4-chloro-3-indolyl-β-D-galactopyranoside, and counterstained with hematoxylin. MetaVue image analysis software (Universal Imaging Corp.) was used to quantify virally infected areas on 10 to 20 slides that collectively covered the entire tumor.

Gene expression analysis. Total tumor RNA was extracted with Trizol reagent (Invitrogen) following the manufacturer's guidelines. cDNA was synthesized from 2 μg total RNA using the Omniscript Reverse Transcriptase kit (Qiagen). cDNA samples were diluted 1:100 in water for quantitative real-time PCR. PCR was done in 25 μL aqueous solution containing 0.9 μmol/L of each primer, 0.2 μmol/L of 5′VIC-3′TAMRA–labeled probe, 12.5 μL of 2× Universal Master Mix (Applied Biosystems), and 5 μL of diluted cDNA using the ABI Prism 7900 HT Sequence Detection System (Applied Biosystems). PCR included 2 min at 50°C, 10 min at 95°C, and 40 cycles at 95°C for 15 s followed by 1 min at 60°C. *LacZ* cDNA amplification was done in triplicate, with *β-actin* as internal control. *LacZ* expression was quantified with the formula $2^{\Delta Ct\ \text{test gene}}/2^{\Delta Ct\ \text{actin}}$; *C*t is the number of cycles at which saturation is reached, and Δ*C*t is the difference between the number of cycles needed to reach saturation for a gene of a tumor from rats treated with virus alone (used as baseline) and from rats treated with virus and an immunosuppressive drug (CL or CPA). The

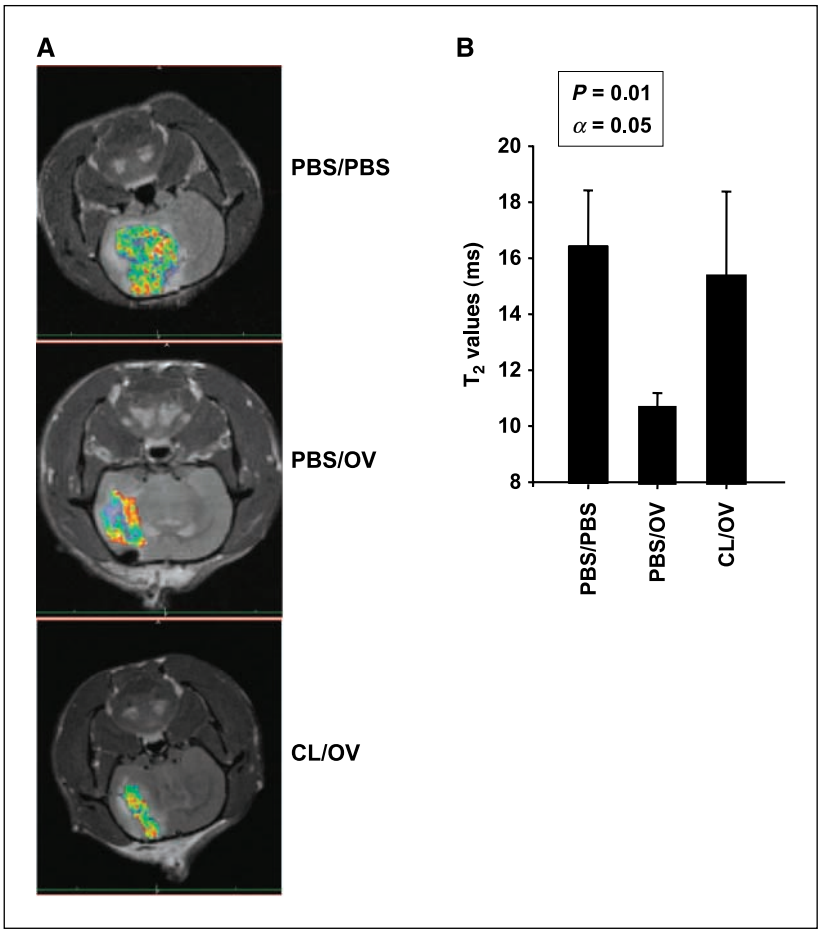

Figure 1. MR imaging and quantification of tumor-associated phagocytic cells. *A,* tumors of animals treated with mock solution (*PBS/PBS, top*), intratumoral OV (*PBS/OV, middle*), or CL (*CL/OV, bottom*) before intratumoral OV were imaged for peripheral macrophages infiltrating the tumor. Imaging was done 72 h after OV injection. MR signals were color coded. *Shift toward red,* decreased T_2-weighted signal; *shift toward blue,* increased signal. The darker the T_2-weighted signal, the more superparamagnetic iron oxide particles are incorporated in the tumor by infiltrating peripheral phagocytic cells. *B, columns,* mean T_2 value (expressed in milliseconds) from 16 images of three rats per treatment group; *bars,* SD. Higher T_2 values correspond to decreased intratumoral infiltration of peripheral macrophages. Significance of pair means comparison was determined by ANOVA followed by post hoc Tukey's test (n = 3).

primers and probes for each gene were designed with the Primer Express program (Applied Biosystems). The primers were as follows: β-actin, ctacagatcatgtttgagaccttcaac (forward), ccagaggcatacagggacaac (reverse), and cagccatgtacgtagccatccaggct (probe); LacZ, aatggctttcgctacctgga (forward), ccatcgcgtgggcgta (reverse), and cgcccgctgatcctttgcga (probe).

Viral yield assay. Titers of infectious viral particles recovered from virus-inoculated rat brains were measured as follows. Freshly removed cerebra were placed in 2 mL DMEM supplemented with a penicillin-streptomycin solution (Cellgro), manually homogenized, and frozen and thawed for three cycles. After final thaw, the lysate was sonicated for 10 s to ensure release of the virus. Cellular debris was then pelleted by centrifugation. Virus-containing supernatant was collected before titration on green monkey kidney cells (VERO) by plaque formation. The same procedure was applied to brain slices grown *in vitro*.

Statistical analysis. ANOVA followed by means comparisons with post hoc Tukey's test established statistical significance.

Results

CLs cause pharmacologic depletion of intratumoral macrophages *in vivo*. We have shown that CPA treatment before OV inoculation of rats carrying syngeneic gliomas significantly increased viral replication capacity and intratumoral persistence (24, 25, 27). These phenomena were associated with CPA-mediated inhibition of intratumoral infiltration of different cells of monocytic lineage (monocytes, microglia, and macrophages) and decreased intratumoral concentration of phagocytic cells (31, 32). To analyze the effect of phagocytic cells on OV intratumoral propagation during virotherapy, we pretreated animals with CL. CLs are efficiently taken up by phagocytic cells, and the intracellular release of clodronate sodium during enzymatic breakdown of the liposomes within the macrophages causes apoptosis and selective depletion of these cells (41). CLs do not cross the blood-brain barrier (data not shown), so they cannot deplete brain-resident phagocytic microglia when delivered systemically.

We analyzed CL-mediated intratumoral depletion of phagocytic cells using a molecular imaging technique that was previously shown to monitor the intratumoral OV-induced infiltration of macrophages (31). We targeted macrophages with i.v. administered dextran-coated iron oxide particles [monocrystalline iron oxide nanoparticle (MION); ref. 42]. MIONs are incorporated by and provide superparamagnetic properties to phagocytic cells, enabling MR imaging. We thus imaged rodent brain tumors as a function of OV and CL treatment. OV treatment significantly decreased T_2-weighted signal (Fig. 1, *shift toward red*), which reflected increased magnetic susceptibility and corresponded to more intratumoral MION-loaded macrophages. Pretreatment with CL reduced magnetic susceptibility to basal levels, thereby inhibiting the capacity of phagocytic cells to infiltrate brain tumors infected by OV.

Identification of cells depleted by CL treatment. We have shown that intratumoral injection of OV causes infiltration of $CD68^+$ and $CD163^+$ monocytes/microglia/macrophages and that treatment with CPA before OV delivery inhibits this phenomenon (31). To evaluate which of these two monocytic cell lineages were depleted by CL, we did FACS and immunohistochemical analysis

on brains harvested from rats with established gliomas (Fig. 2). Three treatment groups were compared: control animals receiving mock solution (PBS), animals receiving PBS and OV, and animals receiving CL and OV.

FACS analysis of the entire hemisphere harboring the tumor showed a doubling of intratumoral $CD68^+$ and $CD163^+$ cells following OV injection; treatment with CL depleted OV-induced $CD163^+$ cells but not $CD68^+$ cells (Fig. 2*A*; Supplementary Fig. S1). Immunohistochemical analysis of brains with tumors harvested from animals undergoing the same treatment regimens confirmed these data (Fig. 2*B*; Supplementary Fig. S2). Qualitatively, $CD68^+$ cells seemed concentrated around the tumor border, whereas $CD163^+$ cells were spread within the tumor (Fig. 2*B*). CL treatment also seemed to increase concentration of $CD68^+$ cells at the tumor periphery, but FACS quantification revealed no statistically significant increase in overall $CD68^+$ cells in CL-treated animals (Fig. 2*A*).

FACS analysis of peripheral blood mononuclear cells (data not shown) and spleen (Supplementary Fig. S3) extracted from animals with established gliomas and treated with either OV alone or CL and OV combined confirmed that CL depleted $CD163^+$ and not $CD68^+$ cells. This and the intratumoral distribution of these two monocytic cell types suggested that $CD163^+$ cells were phagocytic macrophages infiltrating the tumor from the periphery, whereas the observed $CD68^+$ cells could be peripheral monocytes with no phagocytic activity and/or brain microglia with possible phagocytic activity (43, 44).

To further evaluate the phagocytic activity of $CD68^+$ and $CD163^+$ cells, we did laser scanning confocal microscopy on rat tumors 3 days after OV treatment (Fig. 2*C*; Supplementary Fig. S4). This

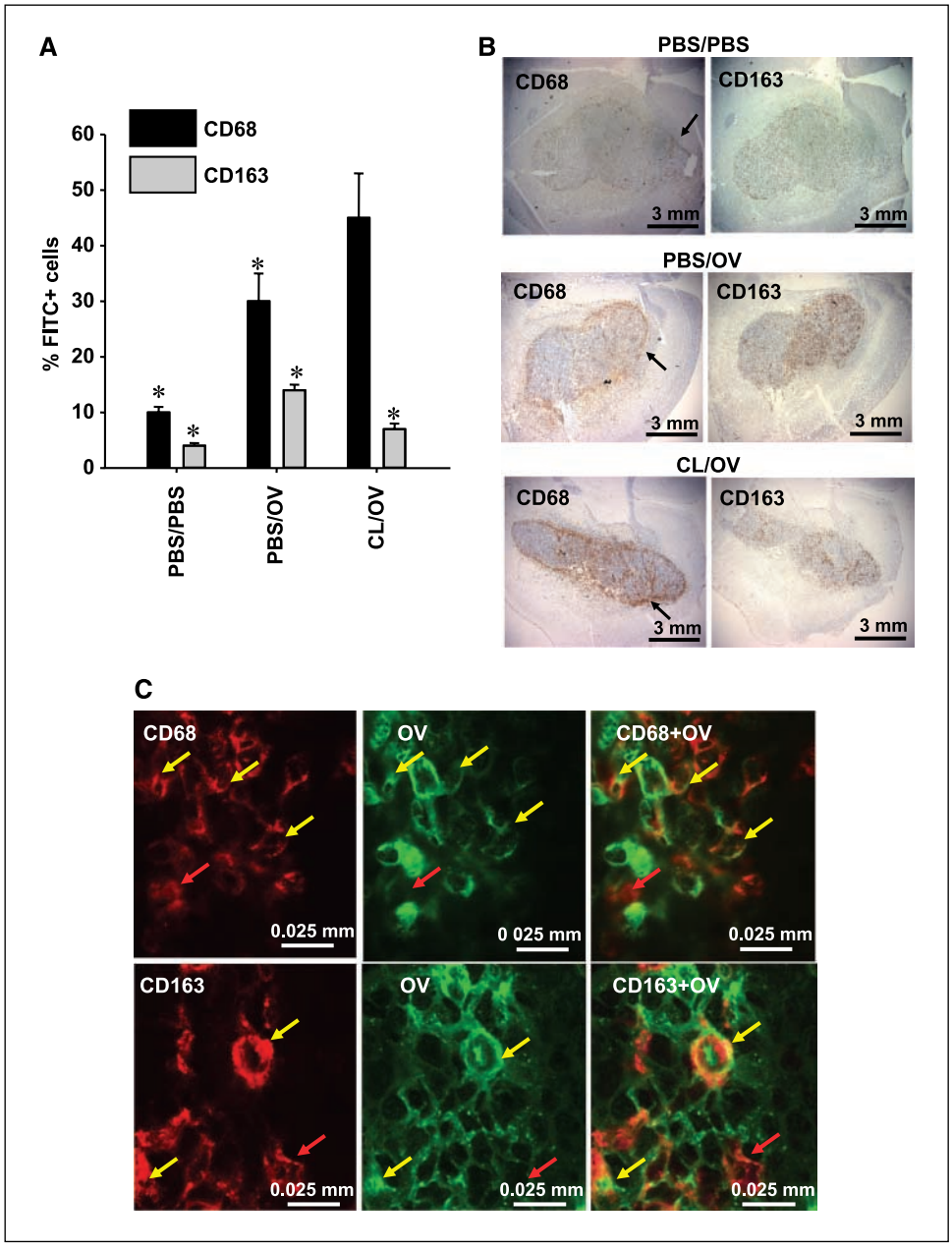

Figure 2. CL-mediated depletion of tumor-associated phagocytic cells. *A,* FACS analysis of the brain hemispheres harboring gliomas from rats treated with mock solution (*PBS/PBS*), OV alone (*PBS/OV*), or CL (*CL/OV*) before OV delivery. The graph shows the average percentage of $CD68^+$ and $CD163^+$ cells, detected by FACS, within the whole brain hemisphere of each treatment group ($n = 3$). For each cell type, a 3-fold increase is observed following OV treatment, and this increase is inhibited by CL treatment only for $CD163^+$ cells. Significance of pair means comparison was determined by ANOVA followed by post hoc Tukey's test for each cell type (CD68: $P = 0.0085$; CD163: $P = 0.011$). *Asterisks,* significant differences. No significant difference was observed for $CD68^+$ cells in animals treated with PBS/OV and CL/OV. *B,* microphotographs of brains with established D74/HveC syngeneic gliomas for rats treated with mock vehicle (*PBS/PBS, top row*), OV alone (*PBS/OV, middle row*), and CL (*CL/OV, bottom row*) before OV injection. CL-mediated macrophage depletion is observed only for the CD163 antigen (*right column*), whose intratumoral distribution varies somewhat from that of the $CD68^+$ cells (*left column*). *Black arrows,* accumulation of $CD68^+$ cells around the tumor edge. *C,* microphotographs of OV-infected cancer cells in a rat tumor treated with OV for 72 h. The brains were stained with antibodies recognizing HSV1 antigens (*green*) and either anti-CD68 or anti-CD163 antibodies (*red*). Clones of OV-infected cancer cells are surrounded by $CD68^+$ and $CD163^+$ cells. Some of these are localized in the proximity of HSV and remain red (*red arrows*), but others have clearly incorporated HSV-infected cells, and colocalization of the two markers gives an orange-yellow staining (*yellow arrows*). The incorporation of HSV1 into either $CD68^+$ or $CD163^+$ cells was confirmed by scanning the laser through the slide with 1-μm intervals.

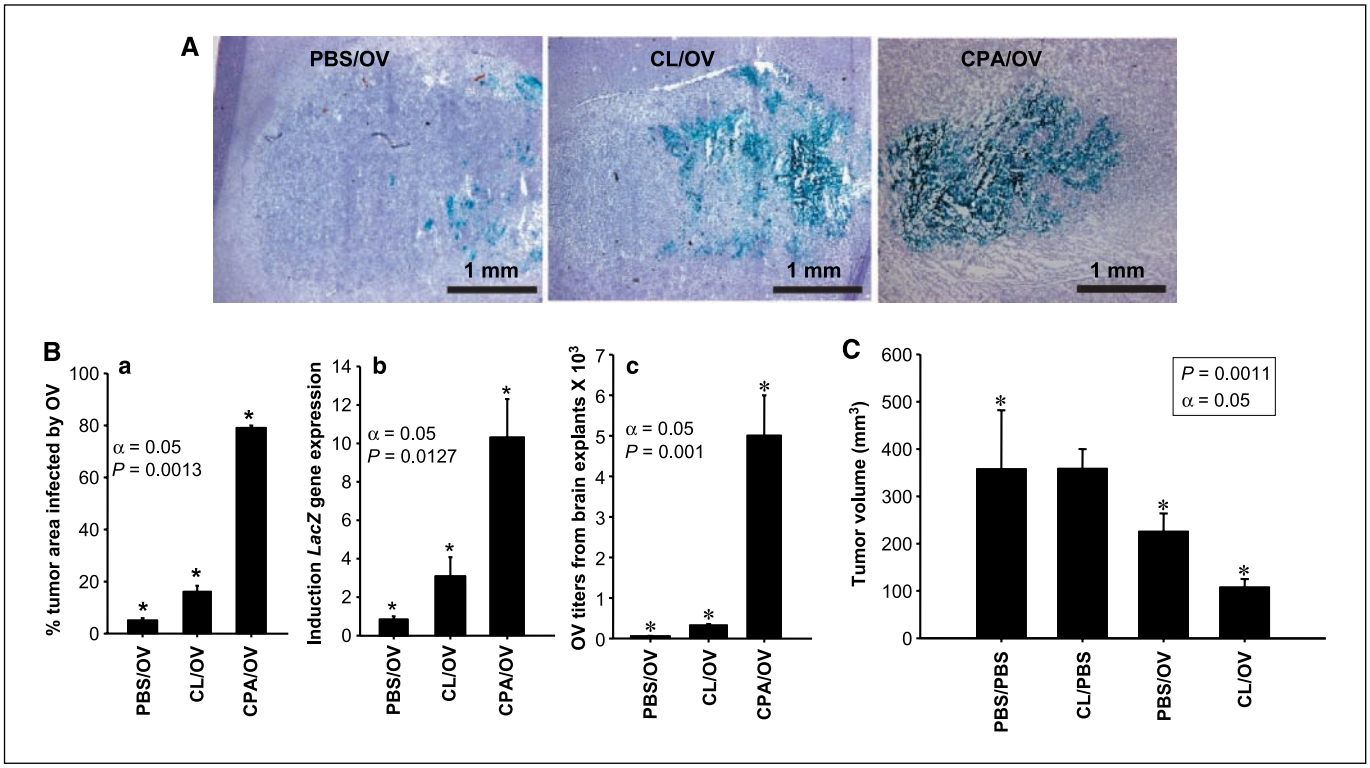

Figure 3. Effects of macrophage depletion on intratumoral spread of OV and tumor size. *A,* intratumoral OV-mediated *LacZ* transgene expression in animals treated with PBS (controls; *PBS/OV*), CL (*CL/OV*), and CPA (*CPA/OV*) before OV delivery. The microphotographs represent the tumor area within the brain hemisphere (purple hematoxylin counterstaining) and *LacZ* transgene expression within the tumor (blue staining for β-galactosidase activity). *B, a, columns,* mean percentage of tumor area infected by OV from the treatment groups described in *A*; *bars,* SD. This experiment was repeated thrice, and one representative result is shown. Significance of pair means comparison was determined by ANOVA followed by post hoc Tukey's test ($n = 4$). *Asterisks,* significant differences. *b,* quantitative RT-PCR for the transcript encoding *LacZ* gene. *Columns,* mean fold induction ($n = 4$) for the transcript encoding *LacZ* in tumors of rats treated with OV alone (controls; *PBS/OV*), both CL and OV (*CL/OV*), and CPA and OV (*CPA/OV*); *bars,* SD. The baseline value of one was attributed to the expression of each gene in control gliomas, and the increase in *LacZ* expression was evaluated (Materials and Methods). The experiment was repeated thrice; one representative experiment is shown. *Asterisks,* means comparisons done with Tukey's test showed significant difference among the three treatment groups. *c,* viral titers from tumors treated with PBS and OV (controls; *PBS/OV*), CL and OV (*CL/OV*), and CPA and OV (*CPA/OV*) were quantified on VERO cells ($n = 8$). *Columns,* average of OV titers obtained; *bars,* SD. Viral titers of animals pretreated with CL increased 5-fold compared with those of animals treated with OV alone, whereas those treated with CPA increased 100-fold compared with control tumors. *Asterisks,* means comparisons done with ANOVA followed by a post hoc Tukey's test showed significant difference between the three treatment groups. *C,* brain tumor volume (mm^3) was measured by MR imaging in animals treated with mock solution (*PBS/PBS*), CL alone (*CL/PBS*), OV alone (*PBS/OV*), and CL and OV (*CL/OV*); $n = 3$. *Asterisks,* comparisons of the means with Tukey's test showed significant changes, with $\alpha = 0.05$ among the three pair comparisons. No significant difference was present between PBS/PBS and CL/PBS treatment groups.

analysis showed that $CD68^+$ and $CD163^+$ cells surround virus-infected tumor cells and contain viral-expressed antigens. Thus, both $CD163^+$ and $CD68^+$ cells seem to have phagocytic activity in the tumor.

Comparison of OV intratumoral proliferation, spread, and persistence in animals pretreated with PBS, CPA, or CL. To understand how peripheral $CD163^+$ macrophages affected glioma virotherapy, we tested if treatment with CL before virus injection would efficiently enhance intratumoral OV proliferation and mimic the effects previously shown with CPA (31) in rats harboring gliomas. The anatomic volume of infected tumor in animals 72 h following viral delivery averaged 4% in the absence of immunomodulation but increased to 16% when animals were pretreated with CL and to 80% when pretreated with CPA (Fig. 3*A* and *B*). Quantitative real-time reverse transcription-PCR (RT-PCR) confirmed this for intratumoral OV-mediated *LacZ* transgene expression. *LacZ* gene expression was thrice greater in animals pretreated with CL than in control rats receiving only OV, a smaller difference than the 10-fold increase in expression observed with CPA administration (Fig. 3*B*). CL effects on intratumoral viral persistence were also evaluated by titrating viral particles from the explanted tumors. Figure 3*B* shows that CL treatment induced a 5-fold increase in viral titers and CPA induced a 100-fold difference. The limited capacity of CL to replicate CPA effects on OV replication was also found sufficient to halve tumor size (Fig. 3*C*) but not to affect animal survival (data not shown; ref. 27).

Therefore, these results showed that selective depletion of the peripheral $CD163^+$ macrophages only partially recapitulated the effect of CPA on OV replication.

CL causes depletion of microglial cells and increase in OV titers on *ex vivo* brain slices. To verify if tumor-associated $CD68^+$ cells are phagocytic brain microglia, we established syngeneic D74/HveC gliomas on rat brain slices grown *ex vivo*. Immunofluorescent staining of the slices before and after OV infection showed that OV induced intratumoral infiltration of $CD68^+$ cells normally surrounding the tumor (Fig. 4; Supplementary Fig. S5). $CD163^+$ cells were not present in these tissues (Fig. 4), in agreement with the fact that CD163 is an antigen for peripheral macrophages in rats (45). CL treatment before virus infection depleted most $CD68^+$ cells from the whole-brain slice (Fig. 4; Supplementary Fig. S5). These data clearly indicate that tumor-associated $CD68^+$ cells are brain microglial cells with phagocytic activity responsible for rapid viral clearance.

We then evaluated the capacity of CL to increase intracerebral viral titers on brain slices with established D74/HveC gliomas and treated with PBS or CL before OV. OV particles extracted from rat brain slices were titered on VERO cells at 3, 5, and 8 days after infection (Fig. 5*A*). Three days after viral treatment, we observed a 5-fold decrease in OV titers explanted from the control slices. Five days after infection, a 10-fold difference was observed between PBS- and CL-treated brain slices. Indeed, in CL-treated slices, OV titers increased from 50 initial pfu (virus input at day 0) to $\sim 10^3$ pfu, whereas in PBS-treated slices an average of 80 OV pfu was explanted. Eight days after OV infection, the difference between the two treatment groups had decreased to 5-fold.

Similar results were obtained in brain slices from athymic *nu/nu* mice implanted with human glioblastoma X12 cells (39) and infected with rQNestin34.5 HSV-derived OV (40). Green fluorescent protein (GFP) expression revealed increased virus in CL-treated compared with PBS-treated (control) brain slices (Fig. 5*B*).

Brain slices not implanted with tumor spheroids were used as an additional control and presented sparse OV-infected cells and no significant viral replication (data not shown). These data indicate that depletion of $CD68^+$ microglial cells increases intratumoral OV titers within brain slices grown *ex vivo* and that this phenomenon is not species or viral strain specific. Titers were increased in rats and mice, respectively harboring rat and human gliomas infected with HSV1 OV derived from strains KOS (hrR3) and F (rQNestin34.5).

Intratumoral $CD68^+$ and $CD163^+$ macrophages are present in human gliomas following OV treatment. To determine the relevance of our discoveries, we analyzed the presence of monocytic cells in glioma specimens of patients treated with oncolytic adenovirus and in a brain specimen of a patient affected by HSV1-induced encephalitis.

From the pathologic archives of Massachusetts General Hospital, we obtained specimens of glioma from a patient before and after treatment with ONYX-015, an oncolytic adenovirus (2, 14). Figure 6*A* shows increased CD68 and CD163 immunopositivity in the glioma after ONYX-015 treatment, which was confirmed in a second ONYX-015–treated human glioma (data not shown). Eight random samples of malignant glioma were used as controls, none with significant positivity for $CD68^+$ and $CD163^+$ cells (data not shown).

Because we studied an oncolytic herpes virus and not an adenovirus in the animal model and because human tumors before and after treatment with oncolytic HSV were not readily available, we also analyzed tissue from the brain of a patient affected by HSV1-induced encephalitis. Figure 6*B* shows immunopositivity for CD68 and CD163 in cells that infiltrated the infection site. Thus, the $CD68^+$ and $CD163^+$ cells that inhibit OV spread and persistence in mice and rats are also activated by virotherapy in glioma patients.

Discussion

The advent of OV therapy raised expectations for improved brain tumor treatments, but therapeutic benefit has not been convincing (10–17). However, the strong biological rationale of this strategy underlies continuous laboratory restudy and new clinical trials. The major barrier to virotherapy efficacy has been the inability to induce efficient intratumoral viral distribution. This is a common obstacle in brain tumor therapies but one unexpected with OVs because of their theoretical potential to replicate within cancer cells and spread throughout tumor (17). We and others have suggested that the activation of antiviral immune responses may be one factor responsible for the disappointing intratumoral viral propagation observed *in vivo* and that combined therapy with virus and immunosuppressive agents increased intratumoral

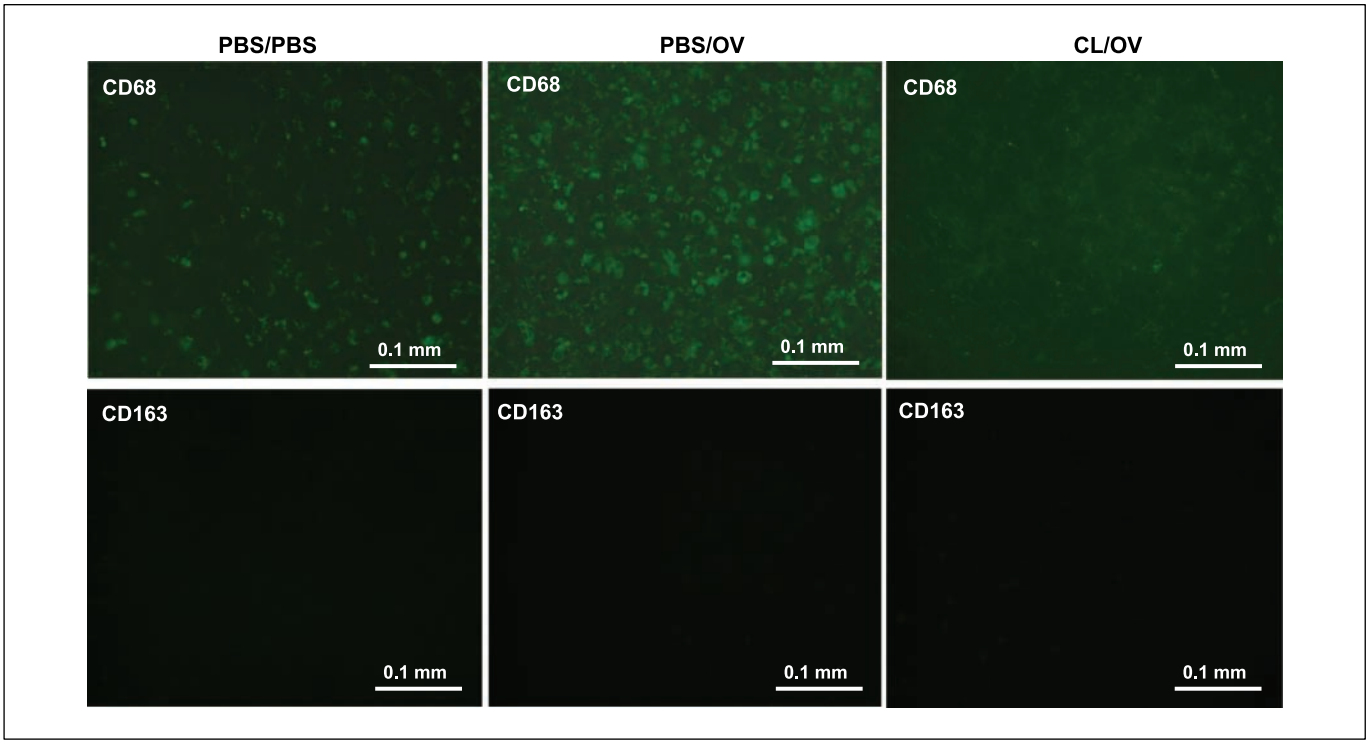

Figure 4. CL-mediated microglia depletion on brain slices cultured *ex vivo*. CD68 (*top*) and CD163 (*bottom*) immunofluorescence in the tumor area of rat brain slices cultured *ex vivo* and treated with mock solution (*PBS/PBS*), mock and OV (*PBS/OV*), and CL and OV (*CL/OV*). The images clearly show OV-mediated intratumoral infiltration of $CD68^+$ cells and their depletion by CL treatment. No $CD163^+$ cells were detected in the whole brain slice, confirming their peripheral origin.

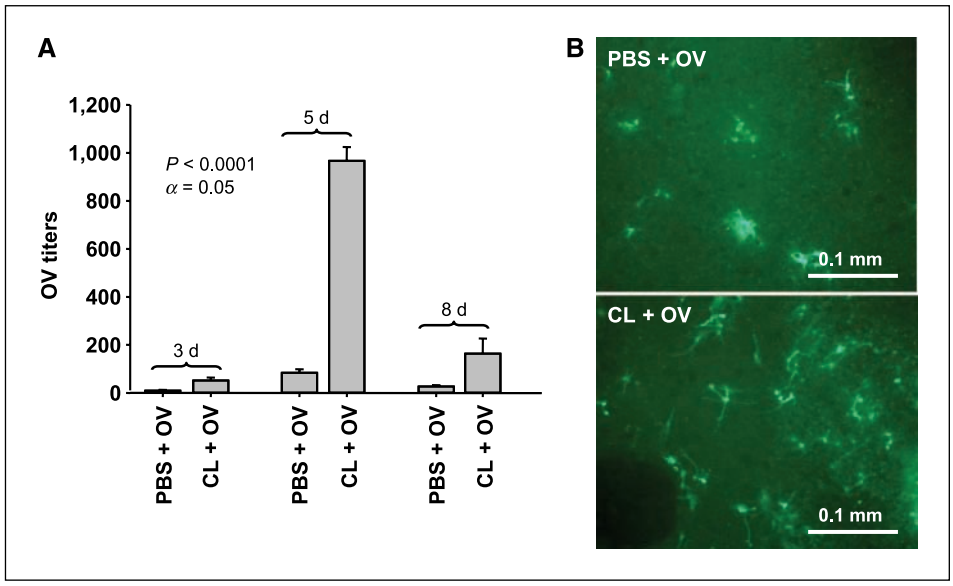

Figure 5. CL-mediated increase in OV titers explanted from *ex vivo* brain slices with established gliomas. *A,* the graph shows the viral titers obtained from brain slices with established D74/HveC gliomas infected with hrR3 OV strain after PBS or CL treatment at 3, 5, and 8 d after virus infection. *Columns,* average of three slices per treatment group; *bars,* SD. The experiment was done twice. Comparison of the means with ANOVA test showed significant changes in virus titers with $\alpha = 0.05$. Post hoc Tukey's test indicated significant changes at each time point between PBS- and CL-treated brain slices. *B,* representative photomicrographs of athymic nude mice brain slices implanted with human X12 glioblastoma cells treated with CL or control. CL-treated slices were thus depleted of resident phagocytes (microglia). rQNestin34.5 was then added to each slice, and its presence was detected by expression of GFP (the transgene is encoded by the virus). Positive signal is indicated by the green fluorescence.

spread and animal survival (24–36). Thus, understanding which innate immune cells inhibit therapeutic effectiveness is necessary to establish a process of selective and transient immunomodulation. In this context, we show for the first time in this report that (*a*) depletion of phagocytic cells enhances intratumoral OV spread, (*b*) both peripheral macrophages ($CD163^+$) and brain microglia ($CD68^+$) contribute to this process, (*c*) this response is not virus and species specific, (*d*) the same cell populations infiltrate the tumors of patients treated with OV, and (*e*) phagocyte depletion partially recapitulates the effect of CPA on enhancing OV replication.

Our research focuses on phagocytic cells based on our preliminary findings of rapid clearance of intratumoral virus particles after OV administration *in vivo* associated with tumor infiltration by cells of monocytic origin (peripheral monocytes, macrophages, or brain microglia; ref. 31, 32). Moreover, on previous analysis of *in vivo* imaging of phagocytic cells infiltrating tumor after OV infection, we observed that this viral clearance was relatively suppressed when animals were treated before viral delivery with CPA, an immunomodulating agent that strongly enhances the intratumoral spread and persistence of OV (31). However, the pleiotropic immunomodulating effects of CPA

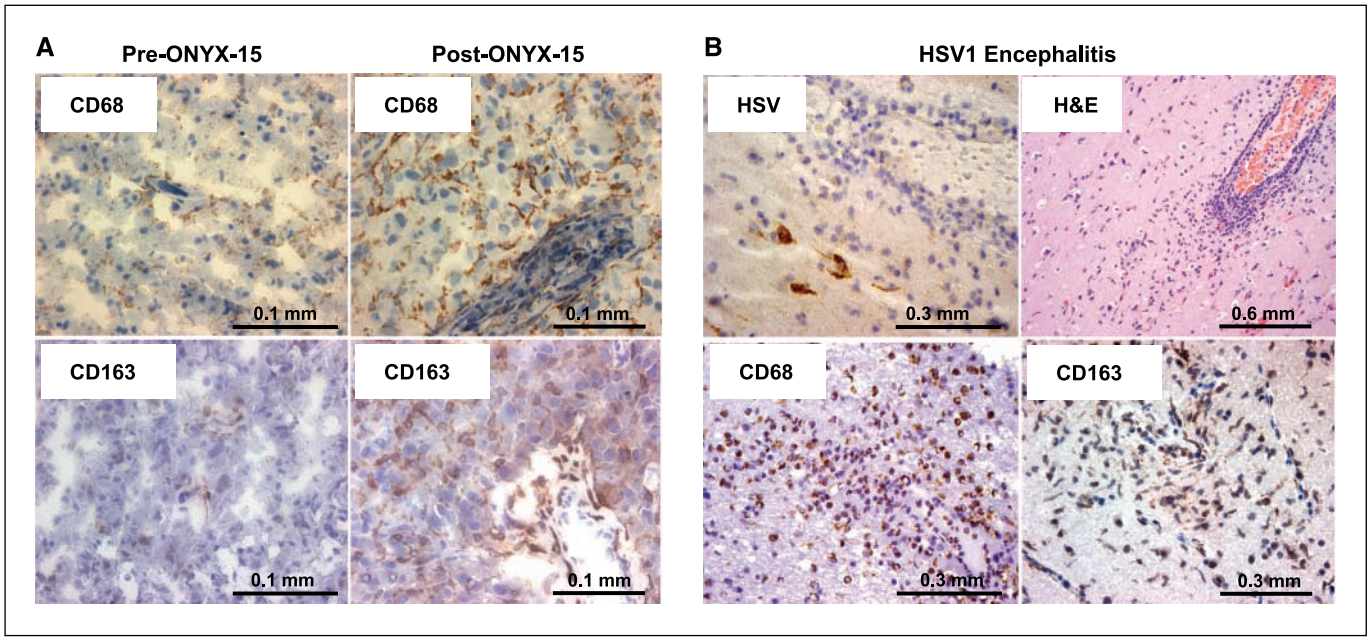

Figure 6. Macrophage infiltration in human brain. *A,* CD68 (*top row*) and CD163 (*bottom row*) immunopositivity in tumors excised from a patient with glioblastoma multiforme before treatment with ONYX-015 (*left column*) and 1 mo after treatment (*right column*). CD68- and CD163-positive cells are indicated by the brown staining over the hematoxylin purple nuclear counterstaining. The figure shows OV-mediated induction of both $CD68^+$ and $CD163^+$ cells in this patient. *B,* the brain from a patient with active HSV1 encephalitis was stained by H&E using antibodies against HSV1 and against the CD68 and CD163 antigens. The figure shows HSV-induced infiltration of $CD68^+$ and $CD163^+$ cells in the brain parenchyma.

prohibited definition of a direct effect of phagocytic cells on intratumoral spread of OV. The use of CL to deplete phagocytic cells selectively and efficiently has been well established (41) and represented a very specific means to understand the role of phagocytic cells in brain tumor virotherapy. Unfortunately, CL cannot cross the blood-brain barrier, so we could deplete peripheral macrophages but not brain-resident phagocytic microglia.

Immunohistochemistry of rat brains harboring syngeneic gliomas with two different macrophage markers showed at least two macrophage/microglial populations. Qualitatively, CD163 antigen appeared on cells dispersed within tumor and in perivascular areas of the brain hemisphere harboring tumor (data not shown), whereas CD68 antigen was also visualized on cells at the periphery of the tumor. These different distribution patterns suggested that we were observing two different monocytic cell types with possibly different origins. Indeed, CD163 antigen is specific for peripheral macrophages in rats and humans (45), whereas CD68 is also described in microglia (44). Moreover, CPA pretreatment depleted both $CD68^+$ and $CD163^+$ cells and led to a 10-fold increase in intratumoral OV (31), but CL depleted only $CD163^+$ cells and increased intratumoral OV only 4-fold. Although tumor size was halved, this was insufficient to increase survival, whereas our former data indicated significantly prolonged animal survival using CPA, which inhibits both $CD68^+$ and $CD163^+$ cells (27, 31) and has other effects.

Brain slices have proved a practical model to study the biology and function of microglial cells and their relation to brain tumor progression (46, 47). We used this experimental model to clarify the molecular and cellular mechanisms that determine the outcomes of experimental brain tumor therapeutics. Although $CD68^+$ cells could be simply nonphagocytic monocytes that inhibit viral replication by releasing IFN-γ and other antiviral cytokines (31, 43), our experiments on brain slices cultured *in vitro* clearly showed the existence of $CD68^+$ phagocytic microglial cells that affected viral propagation, and we observed a 10-fold difference in virus titers between brain slices that were positive and negative for $CD68^+$ cells. These data suggest that CL- and CPA-mediated depletion of both $CD68^+$ and $CD163^+$ cells *in vivo* is associated with increased intratumoral viral titers. Increased intracerebral viral titers in response to CL pretreatment were also observed when we used brain slices derived from athymic *nu/nu* mice implanted with human glioblastoma X12 cells (39) treated with the rQNestin34.5 OV (40). The effects of CPA and CL on intratumoral viral persistence in different animal species and strains, glioma models, as well as viral types indicate that they are not species or virus specific and might be translated to humans. In support of this, $CD68^+$ and $CD163^+$ cells are evident in human gliomas treated with ONYX-015 (1, 7), an adenovirus-derived OV. Further analysis in human gliomas treated with a HSV-derived OV would confirm the relevance of our findings to humans, but lack of such tissue impeded this investigation. However, the presence of $CD68^+$ and $CD163^+$ cells in human brains infected with wild-type HSV suggests evidence supporting this hypothesis. Moreover, recent findings show that CD163 is important in eliminating viral infections of the brain in humans (45).

We have described a deleterious effect of macrophages and microglia in brain tumor virotherapy and suggest future clinical trials using OV in the presence of transient immunosuppression that targets both macrophages and microglia. A similar therapeutic paradigm is being supported for a clinical trial using an oncolytic measles virus in patients with relapsed refractory multiple myeloma.[11] Several chemotherapeutic and anti-inflammatory agents with defined capacity to deplete innate immune cells have been tested preclinically and clinically for glioma therapy and shown dismal therapeutic efficacy (48–50). Our data suggest that the efficacy of these drugs for glioma treatment may be increased if they are used with OV.

[11] A. Dispenzieri, Mayo Clinic, personal communication.

Acknowledgments

Received 3/20/2007; revised 6/2/2007; accepted 7/13/2007.

Grant support: NIH grants PO1 CA69246 and NS41571 and R01 CA85139 (E.A. Chiocca), National Science Foundation grant EEC-02425626 and NIH grant CA095673 (R.L. Martuza), and NIH grant RO1 HL63800 (C.B. Marsh).

The costs of publication of this article were defrayed in part by the payment of page charges. This article must therefore be hereby marked *advertisement* in accordance with 18 U.S.C. Section 1734 solely to indicate this fact.

We thank Farchemia for providing the disodium clodronate used in this study and Rosalyn Uhrig for editorial assistance.

References

1. Martuza RL, Malick A, Markert JM, Ruffner KL, Coen DM. Experimental therapy of human glioma by means of a genetically engineered virus mutant. Science 1991; 252:854–6.
2. Bischoff JR, Kirn DH, Williams A, et al. An adenovirus mutant that replicates selectively in p53-deficient human tumor cells. Science 1996;274:373–6.
3. Alemany R, Balagué C, Curiel DT. Replicative adenoviruses for cancer therapy. Nat Biotechnol 2000;18:723–7.
4. Alemany R, Gómez-Manzano C, Fueyo J. Oncolytic adenovirus for the treatment of cerebral tumors: past, present, and future [in Spanish]. Neurologia 2001;16: 122–7.
5. Kirn D, Martuza RL, Zwiebel J. Replication-selective virotherapy for cancer: biological principles, risk management and future directions. Nat Med 2001;7:781–7.
6. Chiocca EA, Aghi M, Fulci G. Viral therapy for glioblastoma. Cancer J 2003;9:167–79.
7. Fulci G, Chiocca EA. Oncolytic viruses for the therapy of brain tumors and other solid malignancies: a review. Front Biosci 2003;8:e346–60.
8. Dalba C, Klatzmann D, Logg CR, Kasahara N. Beyond oncolytic virotherapy: replication-competent retrovirus vectors for selective and stable transduction of tumors. Curr Gene Ther 2005;5:655–67.
9. Bell JC. Oncolytic viruses: what's next? Curr Cancer Drug Targets 2007;7:127–31.
10. Markert JM, Medlock MD, Rabkin SD, et al. Conditionally replicating herpes simplex virus mutant, G207 for the treatment of malignant glioma: results of a phase I trial. Gene Ther 2000;7:867–74.
11. Rampling R, Cruickshank G, Papanastassiou V, et al. Toxicity evaluation of replication-competent herpes simplex virus (ICP 34.5 null mutant 1716) in patients with recurrent malignant glioma. Gene Ther 2000;7:859–66.
12. Pecora AL, Rizvi N, Cohen GI, et al. Phase I trial of intravenous administration of PV701, an oncolytic virus, in patients with advanced solid cancers. J Clin Oncol 2002;20:2251–66.
13. Lorence RM, Pecora AL, Major PP, et al. Overview of phase I studies of intravenous administration of PV701, an oncolytic virus. Curr Opin Mol Ther 2003;5:618–24.
14. Chiocca EA, Abbed KM, Tatter S, et al. A phase I open-label, dose-escalation, multi-institutional trial of injection with an E1B-attenuated adenovirus, ONYX-015, into the peritumoral region of recurrent malignant gliomas, in the adjuvant setting. Mol Ther 2004; 10:958–66.
15. Csatary LK, Gosztonyi G, Szeberenyi J, et al. MTH-68/H oncolytic viral treatment in human high-grade gliomas. J Neurooncol 2004;67:83–93.
16. Freeman AI, Zakay-Rones Z, Gomori JM, et al. Phase I/II trial of intravenous NDV-HUJ oncolytic virus in recurrent glioblastoma multiforme. Mol Ther 2006;13: 221–8.
17. Fulci G, Chiocca EA. The status of gene therapy for brain tumors. Expert Opin Biol Ther 2007;7:197–208.
18. Toda M, Rabkin SD, Kojima H, Martuza RL. Herpes simplex virus as an *in situ* cancer vaccine for the induction of specific anti-tumor immunity. Hum Gene Ther 1999;10:385–93.
19. Todo T, Martuza RL, Rabkin SD, Johnson PA. Oncolytic herpes simplex virus vector with enhanced MHC class I presentation and tumor cell killing. Proc Natl Acad Sci U S A 2001;98:6396–401.
20. Parker JN, Meleth S, Hughes KB, Gillespie GY, Whitley RJ, Markert JM. Enhanced inhibition of syngeneic murine tumors by combinatorial therapy

with genetically engineered HSV-1 expressing CCL2 and IL-12. Cancer Gene Ther 2005;12:359–68.
21. Parker JN, Pfister LA, Quenelle D, et al. Genetically engineered herpes simplex viruses that express IL-12 or GM-CSF as vaccine candidates. Vaccine 2006;24:1644–52.
22. Varghese S, Rabkin SD, Liu R, Nielsen PG, Ipe T, Martuza RL. Enhanced therapeutic efficacy of IL-12, but not GM-CSF, expressing oncolytic herpes simplex virus for transgenic mouse derived prostate cancers. Cancer Gene Ther 2006;13:253–65.
23. Ino Y, Saeki Y, Fukuhara H, Todo T. Triple combination of oncolytic herpes simplex virus-1 vectors armed with interleukin-12, interleukin-18, or soluble B7-1 results in enhanced antitumor efficacy. Clin Cancer Res 2006;12:643–52.
24. Ikeda K, Ichikawa T, Wakimoto H, et al. Oncolytic virus therapy of multiple tumors in the brain requires suppression of innate and elicited antiviral responses. Nat Med 1999;5:881–7.
25. Ikeda K, Wakimoto H, Ichikawa T, et al. Complement depletion facilitates the infection of multiple brain tumors by an intravascular, replication-conditional herpes simplex virus mutant. J Virol 2000;74:4765–75.
26. Hirasawa K, Nishikawa SG, Norman KL, et al. Systemic reovirus therapy of metastatic cancer in immune-competent mice. Cancer Res 2003;63:348–53.
27. Wakimoto H, Fulci G, Tyminski E, Chiocca EA. Altered expression of antiviral cytokine mRNAs associated with cyclophosphamide's enhancement of viral oncolysis. Gene Ther 2004;11:214–23.
28. Balachandran S, Barber GN. Defective translational control facilitates vesicular stomatitis virus oncolysis. Cancer Cell 2004;5:51–65.
29. Balachandran S, Thomas E, Barber GN. A FADD-dependent innate immune mechanism in mammalian cells. Nature 2004;432:401–5.
30. Lowenstein PR. The case for immunosuppression in clinical gene transfer. Mol Ther 2005;12:185–6.
31. Fulci G, Breymann L, Gianni D, et al. Cyclophosphamide enhances glioma virotherapy by inhibiting innate immune responses. Proc Natl Acad Sci U S A 2006;103:12873–8.
32. Lamfers ML, Fulci G, Gianni D, et al. Cyclophosphamide increases transgene expression mediated by an oncolytic adenovirus in glioma-bearing mice monitored by bioluminescence imaging. Mol Ther 2006;14:779–88.
33. Iankov ID, Pandey M, Harvey M, Griesmann GE, Federspiel MJ, Russell SJ. Immunoglobulin g antibody-mediated enhancement of measles virus infection can bypass the protective antiviral immune response. J Virol 2006;80:8530–40.
34. Friedman A, Tian JP, Fulci G, Chiocca EA, Wang J. Glioma virotherapy: effects of innate immune suppression and increased viral replication capacity. Cancer Res 2006;66:2314–9.
35. Power AT, Bell JC. Cell-based delivery of oncolytic viruses: a new strategic alliance for a biological strike against cancer. Mol Ther 2007;15:660–5.
36. Power AT, Wang J, Falls TJ, et al. Carrier cell-based delivery of an oncolytic virus circumvents antiviral immunity. Mol Ther 2007;15:123–30.
37. Goldstein DJ, Weller SK. An ICP6::lacZ insertional mutagen is used to demonstrate that the UL52 gene of herpes simplex virus type 1 is required for virus growth and DNA synthesis. J Virol 1988;62:2970–7.
38. Del Duca D, Werbowetski T, Del Maestro RF. Spheroid preparation from hanging drops: characterization of a model of brain tumor invasion. J Neurooncol 2004;67:295–303.
39. Giannini C, Sarkaria JN, Saito A, et al. Patient tumor EGFR and PDGFRA gene amplifications retained in an invasive intracranial xenograft model of glioblastoma multiforme. Neurooncol 2005;7:164–76.
40. Kambara H, Okano H, Chiocca EA, Saeki Y. An oncolytic HSV-1 mutant expressing ICP34.5 under control of a nestin promoter increases survival of animals even when symptomatic from a brain tumor. Cancer Res 2005;65:2832–9.
41. Van Rooijen N, Sanders A. Liposome mediated depletion of macrophages: mechanism of action, preparation of liposomes and applications. J Immunol Methods 1994;174:83–93.
42. Moore A, Weissleder R, Bogdanov A. Uptake of dextran-coated monocrystalline iron oxides in tumor cells and macrophages. J Magn Reson Imaging 1997;7:1140–5.
43. Strik HM, Stoll M, Meyermann R. Immune cell infiltration of intrinsic and metastatic intracranial tumours. Anticancer Res 2004;24:37–42.
44. Guillemin GJ, Brew BJ. Microglia, macrophages, perivascular macrophages, and pericytes: a review of function and identification. J Leukoc Biol 2004;75:388–97.
45. Kim WK, Alvarez X, Fisher J, et al. CD163 identifies perivascular macrophages in normal and viral encephalitic brains and potential precursors to perivascular macrophages in blood. Am J Pathol 2006;168:822–34.
46. Markovic DS, Glass R, Synowitz M, Rooijen N, Kettenmann H. Microglia stimulate the invasiveness of glioma cells by increasing the activity of metalloprotease-2. J Neuropathol Exp Neurol 2005;64:754–62.
47. Synowitz M, Glass R, Färber K, et al. A1 adenosine receptors in microglia control glioblastoma-host interaction. Cancer Res 2006;66:8550–7.
48. Tremont-Lukats IW, Gilbert MR. Advances in molecular therapies in patients with brain tumors. Cancer Control 2003;10:125–37.
49. Frazier JL, Wang PP, Case D, et al. Local delivery of minocycline and systemic BCNU have synergistic activity in the treatment of intracranial glioma. J Neurooncol 2003;64:203–9.
50. Weingart JD, Sipos EP, Brem H. The role of minocycline in the treatment of intracranial 9L glioma. J Neurosurg 1995;82:635–40.